17th World Conference on Earthquake Engineering, 17WCEE
Sendai, Japan - September 13th to 18th 2020

EXPERIMENTAL STUDY ON ULTIMATE STATE OF CIRCULARLY PLACED BASE ANCHOR

Y. Shiogama[1], M. Sakai[2] and I. Tamura[3]

[1] *Senior Research Scientist, Central Research Institute of Electric Power Industry, shiogama@criepi.denken.or.jp*
[2] *Senior Research Scientist, Central Research Institute of Electric Power Industry, m-sakai@criepi.denken.or.jp*
[3] *Manager, The Chugoku Electric Power Co., Inc., 350593@pnet.energia.co.jp*
...

Abstract

When assessing seismic performance of base anchor group, yielding of the most stressed anchor is one of criteria for the assessment. But the yielding of one anchor doesn't immediately mean the failure of the whole anchor group. To clarify the behavior of anchor group after anchor yielding, loading test on two anchor group specimens is performed.

Specimens are designed to cause anchor yielding before concrete failure. Each specimen contains the ring base plate which has 850mm of outer diameter, 650mm of inner diameter and 60mm of thickness. On the base plate, 12 anchors which has 13mm diameter and 190mm length, attached circularly. The anchors and some part of base plate are embedded in the base concrete block. The loading jig is fixed on the base plate and loading actuator is connected to the jig with hinge connection. In the loading test, static monotonic loading is applied on one specimen and static cyclic loading is applied on the other specimen.

The test result shows that the load and deformation sufficiently increase after first anchor yielding. From these results, it is considered that the criteria for assessing the seismic performance of the anchor group could accept the further rationalization.

Keywords: seismic performance, anchor, yielding, loading test, monotonic and cyclic loading

© The 17th World Conference on Earthquake Engineering

1. Introduction

In Japan, the margin of seismic resistance of the piping system at nuclear power plants has decreased due to the increase of the reference ground motion. For this reason, it is necessary to establish a rational seismic evaluation method that takes into account nonlinearities such as the elasto-plastic response of structures, and research aimed at upgrading the evaluation method is ongoing.

Vibration tests and earthquake damage cases conducted in the past have shown that damage to the piping system during an earthquake often occurs at locations such as joints of component members and boundaries of support structures. Considering these damage cases, it is necessary to construct a rational evaluation method that considers the ultimate behavior of the boundary part of the equipment such as the foundation anchorage.

In this study, static loading tests were carried out on test specimens simulating the anchoring section in order to construct an earthquake resistance evaluation method considering the elasto-plastic response of the anchoring section. As a result, the ultimate state of the anchoring section where many foundation anchors were arranged was clarified.

2. Loading test

2.1 Test specimen

Fig. 1 shows the outline of the specimen. Fig. 2 and Fig. 3 show the specimen during and after fabrication. The specimen consists of foundation concrete and a base plate with anchors. In this study, two specimens with the same shape were manufactured. The foundation concrete is normal-weight concrete with a design strength of 24N/mm^2 with 17,000 mm in width, 17,000 mm in depth and 500 mm in height. The base plate is a ring with an outer diameter of 850 mm, an inner diameter of 650 mm and a thickness of 60 mm.

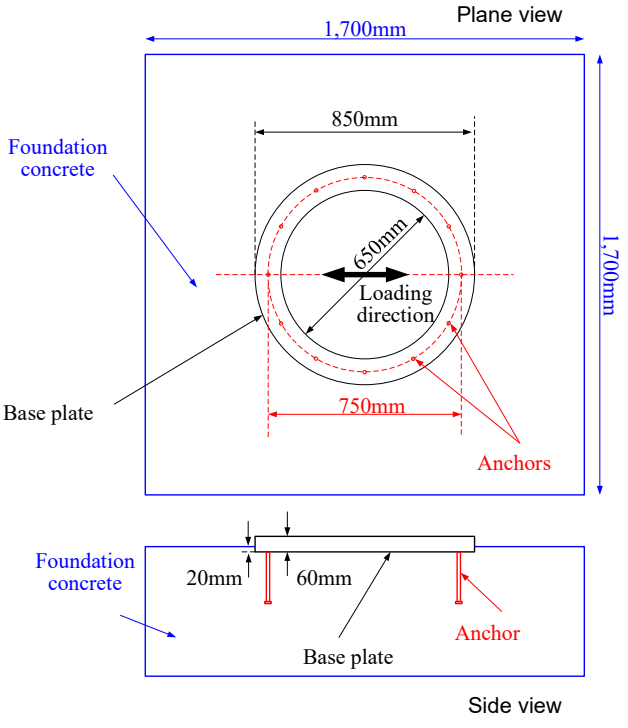

Fig. 1 – Outline of test specimen

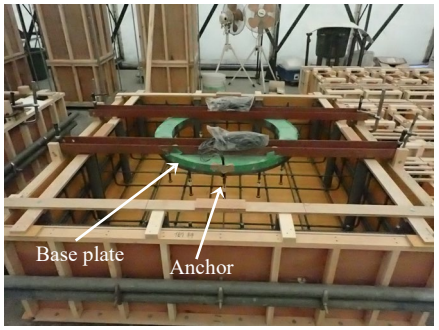

Fig. 2 – Specimen during fabrication

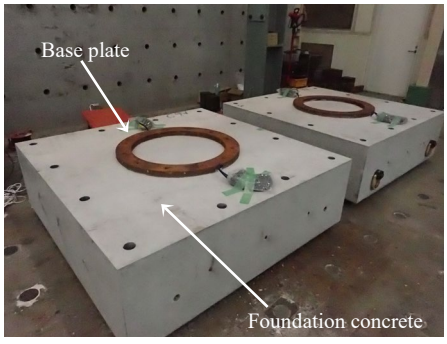

Fig. 3 – Completed specimen

© The 17th World Conference on Earthquake Engineering

On the base plate, twelve anchors are attached at equal intervals in 750 mm diameter circle. The anchors are the headed studs specified in JIS B 1198-2011 [1]. The dimensions of anchor are as follows, axis diameter : 13 mm, head diameter : 25 mm, head thickness : 8.5 mm and length : 190 mm. The bottom 20 mm of the base plate and the anchors are embedded in the foundation concrete.

The strength of the test specimen is designed by referring to the design method described in JEAC4601-2008 [2]. The concrete strength, axis diameter, length and number of anchors are set such that anchor yielding precedes concrete failure.

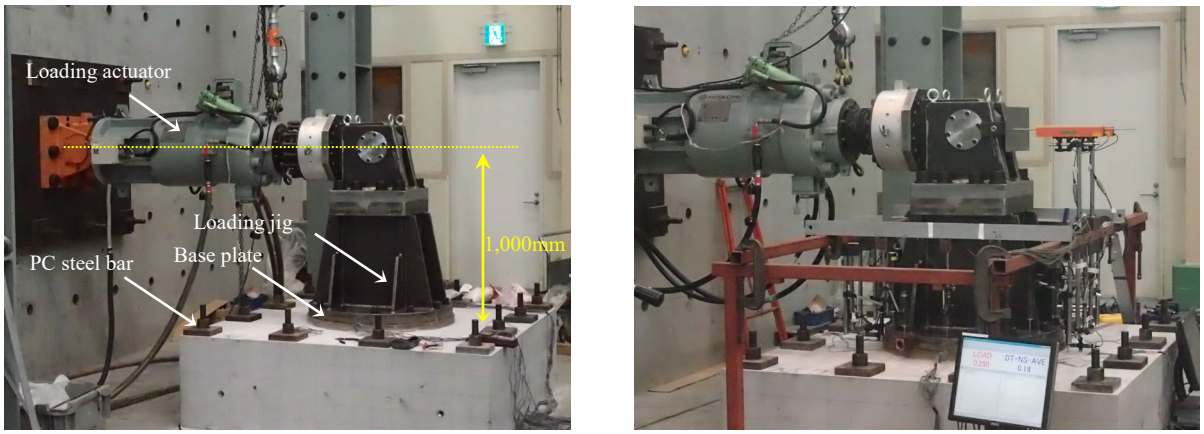

Fig. 4 – Configuretion of loading equipment
Left: before sensor atatchment, right: after sensor atatchment

2.2 Loading method

Fig. 4 shows the outline of the loading test. As shown in the left figure of Fig. 4, the foundation concrete is fixed to the reaction floor with twelve PC steel bars around it. A loading jig is connected to the upper surface of the base plate by high-strength bolts. The upper end of the loading jig is connected to the actuator at a position 1,000 mm from the upper surface of the foundation concrete. In the loading test, monotonic loading and cyclic loading are applied to the specimens, respectively. In the monotonic loading, horizontal displacement is monotonously increased by displacement control. In the cyclic loading, horizontal displacement is applied to the positive and negative alternating by displacement control and the displacement amplitude is increased cycle to cycle.

During the loading test, the following items are measured (see the right figure in Fig. 4).

- Load and displacement of the actuator
- Horizontal displacement at the loading point of the jig
- Horizontal displacement and vertical displacement of base plate
- Horizontal displacement and vertical displacement of foundation concrete
- Anchor strain

Fig. 5 shows the installation of the strain gauge on the anchor. Two uniaxial strain gauges are installed at the center of each anchor axis. Fig. 6 shows the placement of anchors and the loading direction. The actuator is connected from the north side of the specimen. The loading axis is in the north - south direction. The two gauges on each anchor are installed on the forward and backward surfaces in the loading direction, that is, the north and south surfaces. In the following, the bolt located to the north of the specimen will be called "Anchor No.1". The others will be called "Anchor No.2" to "Anchor No.12" for each in clockwise order when viewed from above.

© The 17th World Conference on Earthquake Engineering

Fig. 5 – Strain gages on anchors

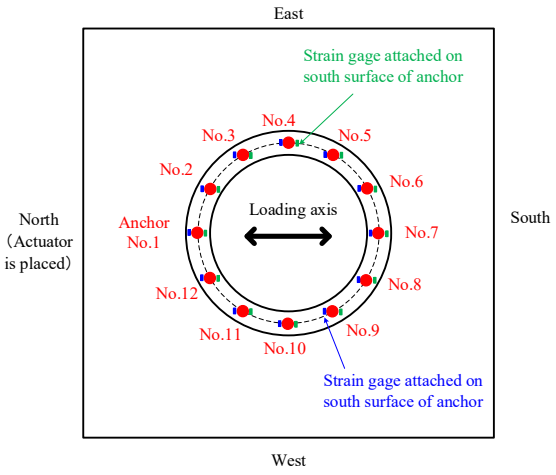

Fig. 6 – Placement of anchors and loding direction

3. Test result

3.1 Result of material test

Tensile tests were performed using three specimens made from the same lot of anchors as the test specimen. Fig.7 shows the stress-strain relations during the tensile test. The average value of the yield stress is 325.8 N/mm^2. This yield stress is 40% larger than 235 N/mm^2 which is the lower limit of yield stress defined in JIS B 1198-2011 [1]. The yield strain obtained by dividing the yield stress by the Young's modulus is 1,571×10^{-6}. This yield strain is a measure of anchor yield during the loading test.

Compression tests were performed using test pieces collected at the time of placing the foundation concrete. Five specimens were tested each on the day of monotonic loading (33 days of age) and on the day of cyclic loading (42 days of age). The average compressive strength is 29.5 N/mm^2 and 30.3 N/mm^2, respectively. This is about 20% greater than the design value of 24 N/mm^2.

As described above, the yield stress of the anchor of the specimen is smaller than assumed in the previous design. And conversely, the compressive strength of the foundation concrete of the specimen is larger than expected in the previous design. Thus, the anchors in test specimens are more likely to yield than expected in the design.

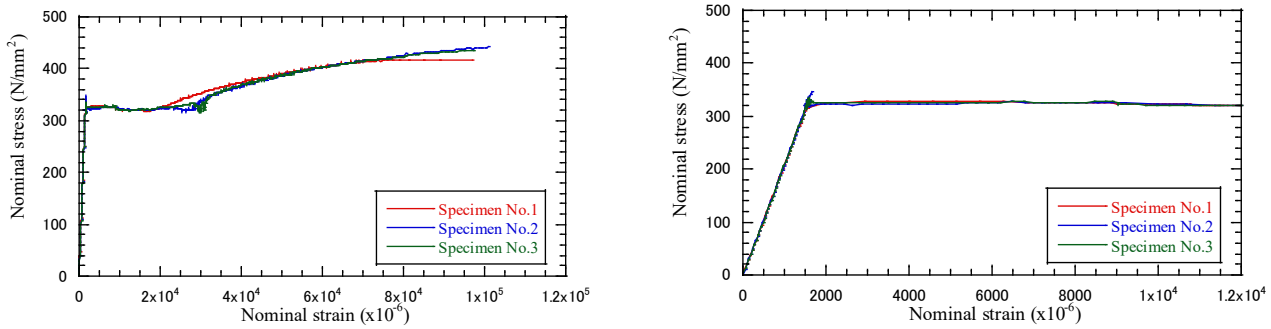

Fig. 7 – Stress-strain relations of anchors in tensile test
Left: whole relations, right: relations around yielding

3.2 Result of monotonic loading test

© The 17th World Conference on Earthquake Engineering

Fig.8 shows the relation between the load and the horizontal displacement at the loading point in the monotonic loading test. The right figure in Fig. 8 is an enlarged part of the left figure. In Fig. 8, the positive side of the horizontal axis is the north direction, that is, the displacement in the direction of pulling by the actuator (see Fig. 6).

As shown in the left figure in Fig. 8, the stiffness of the specimen gradually decreased at around 170 kN while the load increased with increasing displacement, and reached a maximum load of 289.8 kN at 42.95 mm. At the displacement of 53.62 mm (264.1 kN → 231.4 kN), 55.43 mm (224.3 kN → 192.7 kN) and 57.65 mm (188.8 kN → 157.6 kN) after the maximum load, a sharp load drop of about 30 kN occurred with the sound which was considered to be due to anchor break. After that, the loading was continued up to 60 mm and the loading test was completed. When the load reached 100 kN and 200 kN, the loading was interrupted and the state of the test specimen was observed. After that, the loading was interrupted at every 5 mm from 10 mm to 40 mm and at 50 mm, the state of the specimen was observed.

Based on the actual yield stress of the anchor, the yield load at which the Anchor No. 7 at the tensile edge of the moment acting on the specimen starts to yield is calculated as 134.7 kN. The maximum load during the test was 289.8 kN, which was 2.15 times the yield load. From the right figure in Fig. 8, the displacement at the time of yield load was 2.53 mm. The displacement of 42.95mm at the maximum load was about 17 times of the displacement at the yield load.

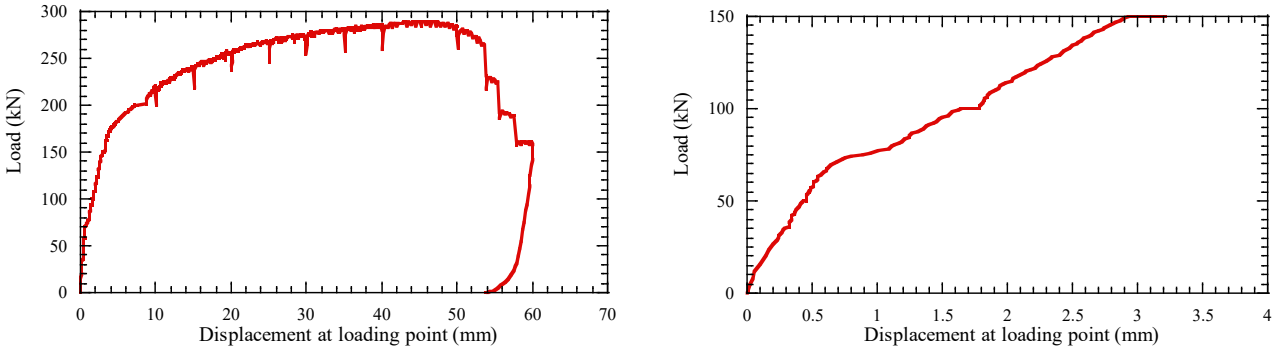

Fig. 8 – Load-displacement relations in monotonic loading test
Left: whole relation, right: relation around anchor yielding

Fig. 9 and Fig. 10 show the relation between the load and strain of each anchor. Each figure includes Anchor No.1 and Anchor No.7 which are on the loading axis. Fig. 9 includes the anchors on the east side of the loading axis. Fig. 10 includes the anchors on the west side of the loading axis. The seven legends in each figure are arranged from north to south in order from the top. The horizontal axis in the figure represents the average value of two strain gauges installed on each anchor. The positive value on the horizontal axis is the tensile strain, and the negative value is the compressive strain. Though a strain exceeding $10{,}000\times10^{-6}$ was observed in the test, the yield strain is shown up to about yielding strain of $1{,}571\times10^{-6}$ in the figures to see the yielding condition of the anchor.

From Fig.9 and Fig.10, at the initial stage of loading, tensile strain was generated in the seven anchors on the south side including Anchor No.4 and No.10 located east and west of the specimen. As the load increased, Anchor No. 7, which was on the southernmost and the tensile end of the moment, reached the yield strain first. Next, it was confirmed that the strain reached the yield strain in order from the anchor on the south side to the anchor on the north side. Though Anchor No. 1, 2, 3, 11 and 12 showed the compressive strain at the beginning of loading, these turned the direction of the strain change to the tensile side as the loading progression. Finally, eleven anchors other than Anchor No.1 yielded.

© The 17th World Conference on Earthquake Engineering

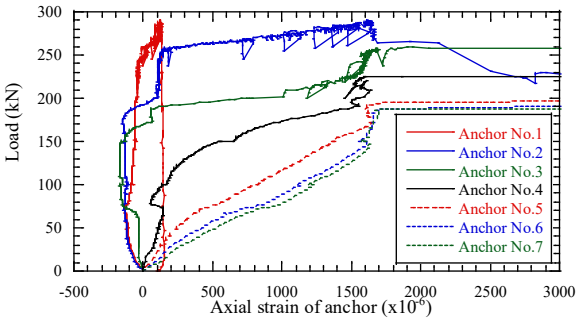

Fig. 9 – Relation between load and strain of anchors(No.1 to No.7) in monotonic loading

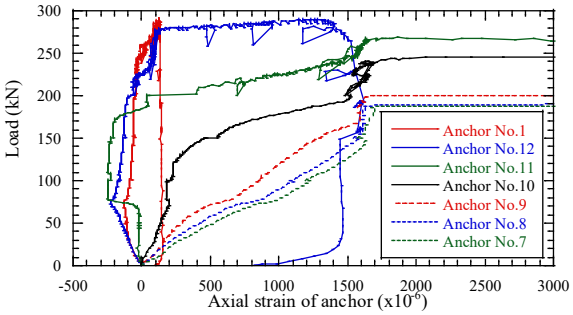

Fig. 10 – Relation between load and strain of anchors(No.1 , No.7 to No.12) in monotonic loading

Fig.11 shows the condition of the test specimen at the maximum displacement of 60 mm during the test. The base plate and the loading jig are tilted to the north, and the south of the base plate is partially raised above the foundation concrete surface. The anchor can be confirmed from the gap between the raised base plate and the foundation concrete.

Fig.12 shows the exposed anchors by removing the foundation concrete after the loading test. These are the three anchors (Anchor No.6, 7 and 8) from the southern end. The necking of the anchor was confirmed near the center of the axis where the strain gauge was attached (see Fig. 12 (a)). Fig.12 (B), (c) and (d) show the close-up around the necking with a fiberscope. All three anchors had been broken. After the maximum load during the test, the load suddenly decreased three times with the sound emission. It is considered that these load reductions and sound emissions are due to the sequential break of Anchor No.6, 7 and 8 as shown in Fig. 12. The order of the anchor break is not clear, but it is probable that Anchor No. 7 at the tensile edge broke first, followed by Anchor No. 6 or Anchor No. 8.

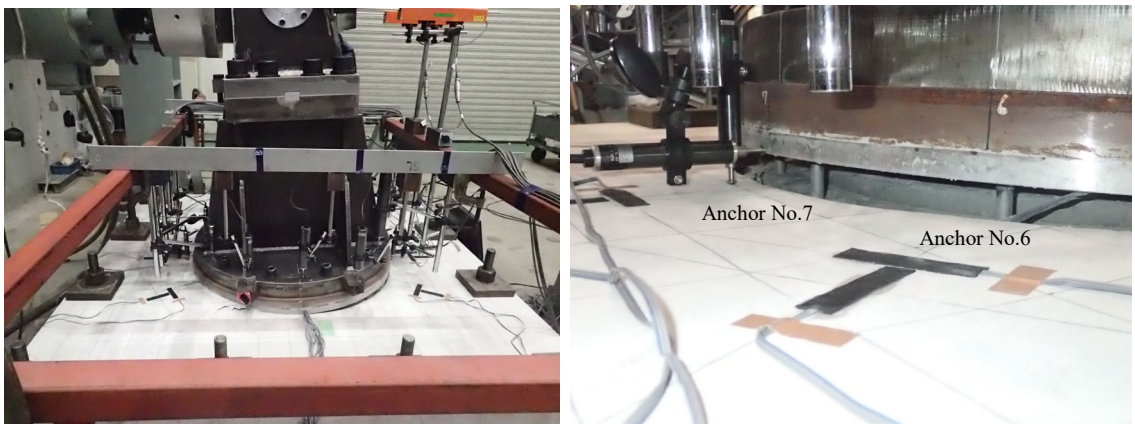

Fig. 11 – Specimen at maximum displacement in monotonic loading test
Right: oberall view, left: near Anchor No.7

© The 17th World Conference on Earthquake Engineering

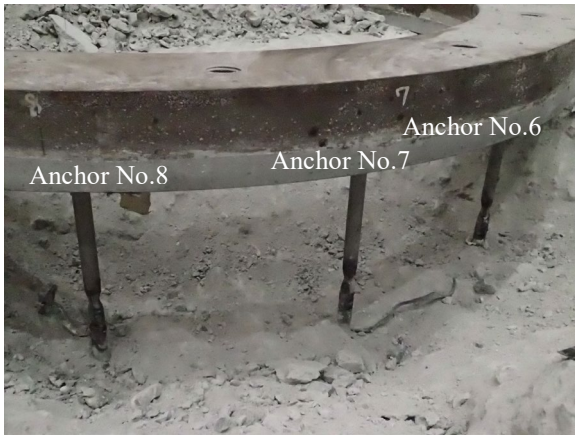

(a) Base plate and anchors

(b) Anchor No.8

(c) Anchor No.7

(d) Anchor No.6

Fig. 12 – Exposed anchors after monotonic loding test

3.3 Result of cyclic loading test

When the horizontal displacement of the loading point reached 2.5 mm, the load reached to the yield load of the anchor at the tensile edge in the monotonic loading test (see Fig. 8). Therefore, this displacement is defined as the yield displacement δ_y (δ_y = 2.5 mm). In the cyclig loading test, the displacement amplitude was gradually increased every cycle as $\pm 1/2\delta_y$, $\pm\delta_y$, $\pm 2\delta_y$, $\pm 4\delta_y$, $\pm 8\delta_y$, $\pm 16\delta_y$, $\pm 24\delta_y$. During one cycle of loading, the loading point was first displaced to the north, that is, toward Anchor No. 1, and then to the south, that is, toward Anchor No. 7. Here, the displacement to the north is defined as a positive displacement, and the displacement to the south is defined as a negative displacement.

Fig. 13 shows the load-displacement relation in thecyclic loading test. Fig. 13 (a) shows the load-displacement relation over the entire test. Fig. 13 (b) is a comparison with the load-displacement relation in the monotonic loading test. Fig. 13 (c) to (h) extract the load-displacement relation for each loading cycle. The arrows in the figures indicate the direction of change from the start of each cycle.

According to Fig. 13, the slip-type restoring force characteristics in which the history returns to near the origin can be confirmed until the third cycle(see Fig.13 (e)). In the fourth cycle(see Fig.13 (f)) and the fifth cycle(see Fig.13 (g)), reversed S-shaped restoring force characteristics gradually appear. In the sixth cycle(see Fig.13 (h)), the reversed S-shaped restoring force characteristic is also exhibited. On the way from + 16δy (= + 40mm) to -16δy (= -40mm) in sixth cycle, a load drop of about 30 kN occurred five times with the sound likely due to anchor break. The sound occurred from -25.50mm to -37.09mm. For the sixth cycle, the loading direction was reversed at -37.09 mm and returned to 0 mm.

Fig. 13 (h) also includes the history of the seventh cycle. In the sventh cycle, load did not recover to the load level of the previous cycle. On the way to +60 mm, the load drop with the sound emission was

© The 17th World Conference on Earthquake Engineering

observed six times from +26.54 mm to +35.15 mm. The amount of load drop was smaller than the five load drops in sixth cycle. In addition, the magnitude of the generated sound was seemed to be smaller than that in the sixth cycle. Finally, a load drop of about 30 kN occurred at +46.64 mm with sound. This is the twelfth sound. Therefore, it was judged that all twelve anchors has broken, and the loading was terminated.

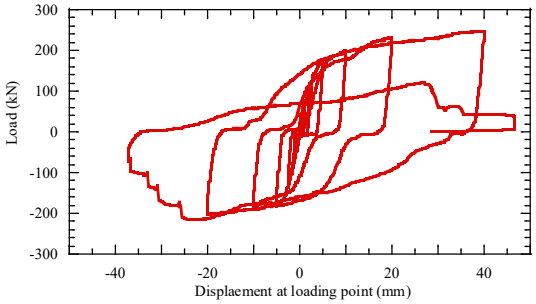

(a) Whole relation

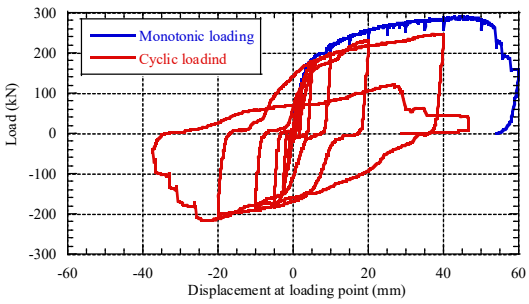

(b) Comparison with monotonic loading

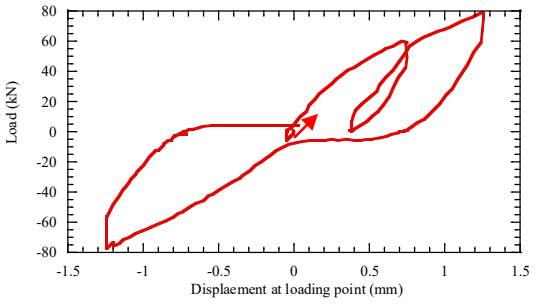

(c) 1st cycle ($\pm 1/2\delta_y = \pm 1.25$mm)

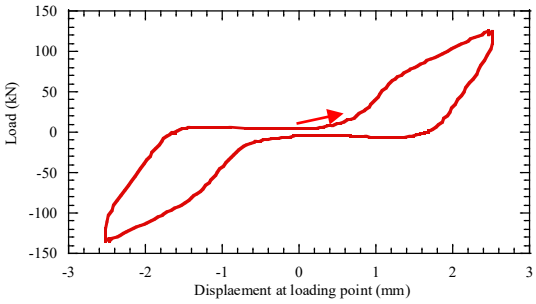

(d) 2nd cycle ($\pm\delta_y = \pm 2.5$mm)

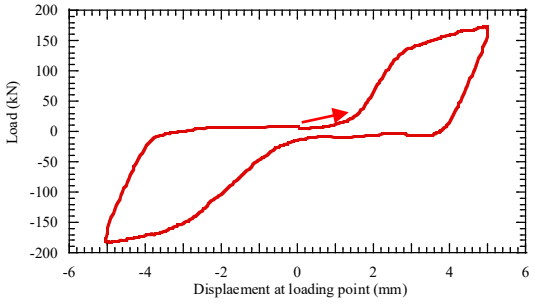

(e) 3rd cycle ($\pm 2\delta_y = \pm 5.0$mm)

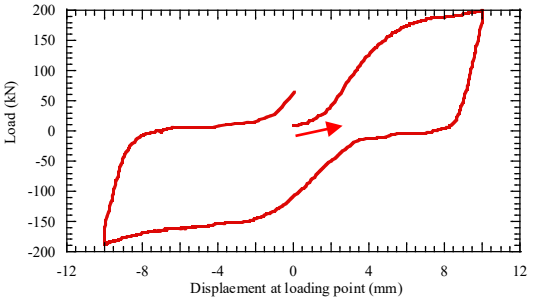

(f) 4th cycle ($4\delta_y = \pm 10.0$mm)

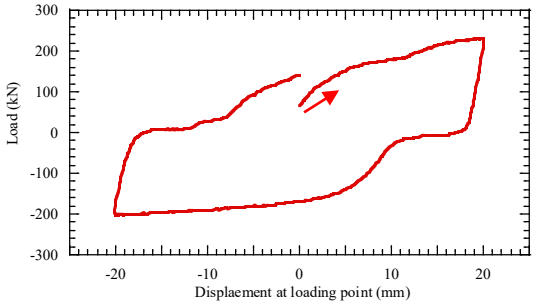

(g) 5th cycle ($\pm 8\delta_y = \pm 20.0$mm)

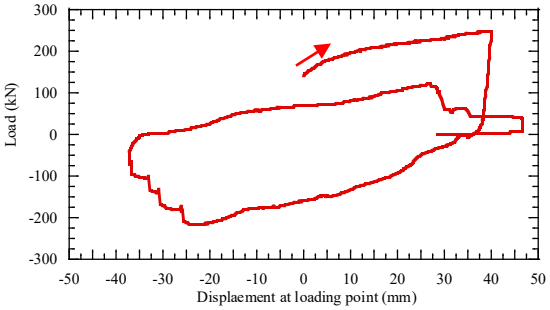

(h) 6th and 7th cycles ($\pm 16\delta_y = \pm 40.0$mm)

Fig. 13 – Load-displacement relation in cyclic loading test

© The 17th World Conference on Earthquake Engineering

Looking at the positive region of the horizontal axis in Fig.13 (b), the skeleton curve up to the sixth cycle of the cyclic loading test shows similar curve with the monotonic loading test. On the negative side of the horizontal axis, the tendency was the same as that on the positive side until the load drop in sixth cycle which was considered to be due to the anchor break.

It is considered that the horizontal displacement at the time of the first anchor break was 53.62mm in monotonic loading test. On the other hand, the first anchor break in cyclic loading test is considered to have occurred at -25.50 mm which was smaller than that of the monotonic loading test.

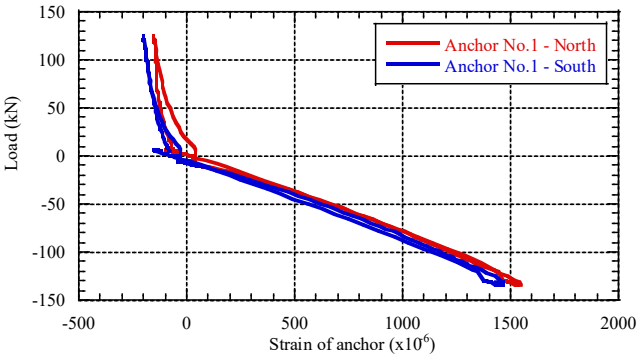

(a) Anchor No.1 in 2nd cycle ($\pm\delta_y$=±2.5mm)

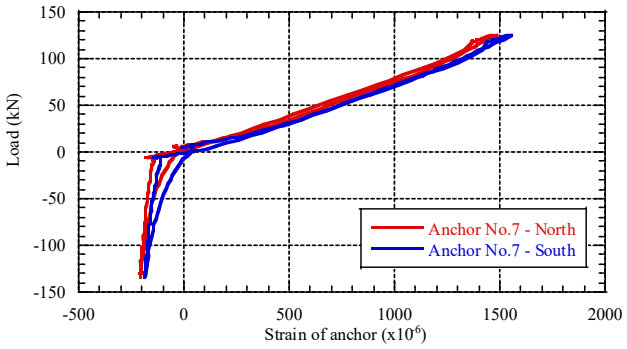

(b) Anchor No.7 in 2nd cycle ($\pm\delta_y$=±2.5mm)

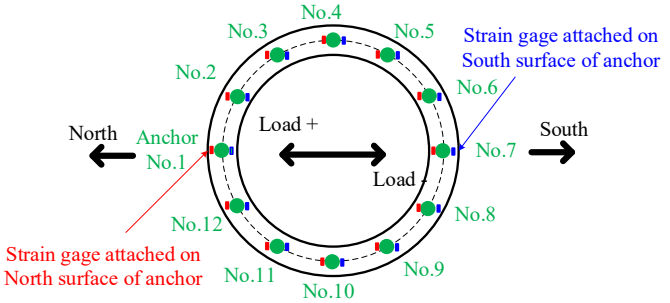

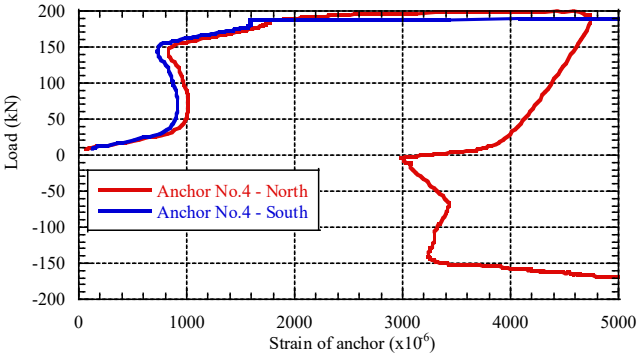

(c) Anchor No.4 in 4nd cycle ($\pm 4\delta_y$=±10.0mm)

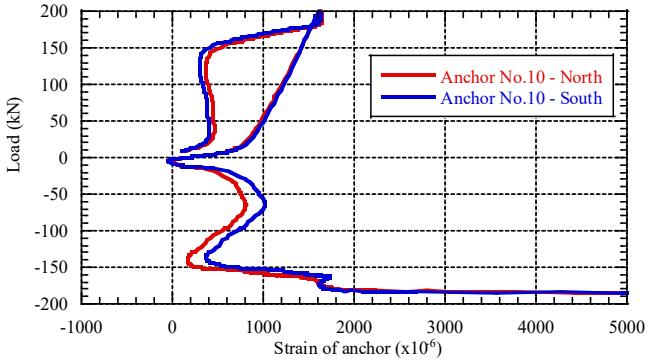

(d) Anchor No.10 in 4nd cycle ($\pm 4\delta_y$=±10.0mm)

Fig. 14 –Relations between load and strain of anchors in cyclic loading test

© The 17th World Conference on Earthquake Engineering

Fig. 14 shows a typical example of the relation between load and anchor strain in cyclic loading test. The horizontal axis in these figures represents the strain of the anchor, where tension is positive and compression is negative. The vertical axis represents the load. The load toward the north is positive and the load toward the south is negative.

Fig. 14 (a) and (b) show the relationship between load and strain of Anchor No.1 and Anchor No.7 in the second cycle ($\pm\delta_y=\pm2.5$mm). When the load is positive, compressive strain occurs in Anchor No. 1 on the north side and tensile strain occurs in Anchor No. 7 on the south side. The magnitude of the strain is small in the compressed anchor. This is assumed to be due to the effect of bearing pressure between the foundation concrete and the bottom suface of the plate. The loading amplitude in the second cycle is the yield displacement in the monotonic loading test. In this cycle, Anchor No.1 and Anchor No.7 each reached the yield strain of $1{,}571\times10^{-6}$.

Fig. 14 (c) and (d) show the relation between load and strain of Anchor No.4 and Anchor No.10 in the fourth cycle ($\pm4\delta_y=\pm10$mm). In Fig. 14 (d), the strain of Anchor No.10 changes only on the tensile side for both positive and negative loads. In addition, since both Anchor No. 4 and Anchor No. 10 reached the yield strain, so it is considered that all anchors yielded by the fourth cycle.

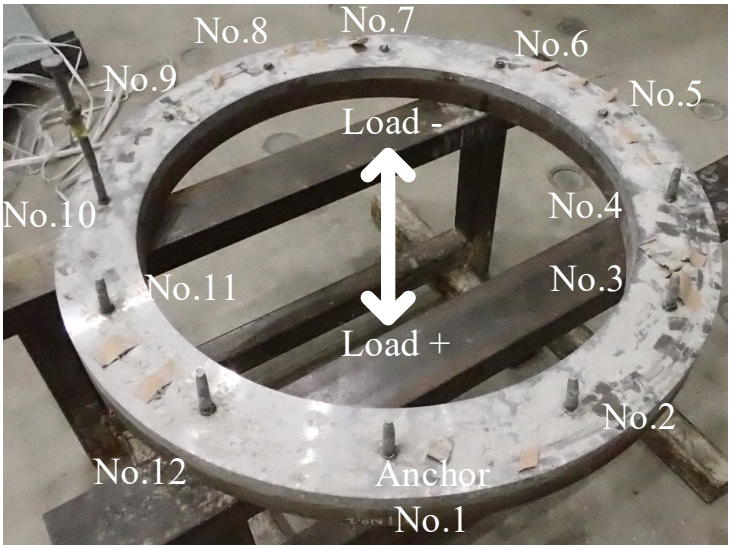

(a) All anchors

(b) Anchor No.10

(c) Anchor No.1

(d) Anchor No.4

(e) Anchor No.5

Fig. 15 – Dameged anchors

© The 17th World Conference on Earthquake Engineering

Fig.15 shows the base plate and anchor that were taken out after the test. Fig. 15 (a) shows the entire lower surface of the base plate, and Fig. 15 (b) to (e) show the condition of each anchor. As shown in Fig. 14 (a), eleven anchors except Anchor No. 10 were broken. Looking at the broken anchors, the broken state is divided into two types. Anchor No.1 to No.4, Anchor No.11 and No.12, which were on the north side at the time of the test, broke at a position of about 40 mm to 50 mm from the lower surface of the base plate. On the other hand, Anchor No. 5 to No.9 on the south side broke near the joint to the lower surface of the base plate.

In the above, it is mensioned that in the sixth cycle (see Fig. 13 (h)), from horizontal displacement of -25.50mm to -37.09mm, the load drop of about 30kN with the sound of anchor break occurred. When the loading point is displaced to the negative side, that is, to the south side, it is the anchor located on the north side that becomes tensile. Therefore, the five breaking sounds generated in this cycle are considered to be any of Anchor No.1 to No.4, Anchor No. 11 and No.12. Assuming that the anchor break occurs sequentially from the tensile edge of the moment, it is probable that five of them except Anchor No. 4 broke in the sixth cycle.

In the 7th cycle, there were six load drops of about 10 kN with smaller sound and finally a load reduction of about 30 kN with larger sound. It is considered that one of the six load drops of about 10 kN accompanied by a small sound was caused by something other than anchor break. It is thought that the remaining five load drops were caused by the break of Anchor No. 5 to No. 9 on the south side.

The load drop of about 30kN accompanied by the last large sound is considered to be due to the break of Anchor No.4 from the similarity of the sound magnitude, the load drop amount and the breaking mode. Since Anchor No. 10 remains without break, it is reasonable to assume that Anchor No. 4 on the opposite side of the loading axis broken last.

4. Conclusion

In this study, static monotonic loading test and static cyclic loading test were performed on a specimen with circularly placed anchors in order to establish an earthquake resistance evaluation method considering the elasto-plastic response of the foundation anchor.

In the monotonic loading test, both the load and displacement continued to increase after the yield load at which the anchor at the tensile edge of the moment yielded. The maximum load was 2.15 times the yield load. The displacement at the maximum load was 17 times the yield displacement δ_y at which the yield load was reached. After the maximum load, break of the anchor began to occur at about $21\delta_y$, and the load decreased sharply with each break.

In the cyclic loading test, the loading point displacement is gradually increased every cycle as $\pm 1/2\delta_y$, $\pm\delta_y$, $\pm 2\delta_y$, $\pm 4\delta_y$, $\pm 8\delta_y$, $\pm 16\delta_y$, $\pm 24\delta_y$, based on the yield displacement δ_y of the monotonic loading test. At $\pm 1/2\delta_y$, $\pm\delta_y$ and $\pm 2\delta_y$, slip-type restoring force characteristics were shown and reversed S-shaped restoring force characteristics were exhibited after $\pm 4\delta_y$ cycle. Some anchors broke during the $\pm 16\delta_y$ cycle and some of the remaining unbroken anchors broke during the $\pm 24\delta_y$ cycle. Two types of anchor break were observed, and the amount of load reduction at the break was different for each.

The circular array of anchors used in the test has large deformation performance and strength even after the yield of some anchors. From these results, it is considered that the criteria for assessing the seismic performance of the anchor group could accept the further rationalization.

References

[1] JIS B 1198:2011 Headed studs.

[2] JEAC 4601-2008:Technical Standard for Seismic Design of Nuclear Power Plant (in Japanese).

© The 17th World Conference on Earthquake Engineering